# Supporting Information

# Non-diffusive transport and anisotropic thermal conductivity in high-density Pt/Co superlattices

*Mohammadreza Shahzadeh[1], Olga Andriyevska[2], Ruslan Salikhov[3], Lorenzo Fallarino[3,†], Olav Hellwig[3,4], Simone Pisana[1,2,*]*

1. Department of Electrical Engineering and Computer Science, York University, 4700 Keele Street, Toronto ON, M3J 1P3, Canada

2. Department of Physics and Astronomy, York University, 4700 Keele Street, Toronto ON, M3J 1P3, Canada

3. Institute of Ion Beam Physics and Materials Research, Helmholtz-Zentrum Dresden-Rossendorf, Bautzner Landstraße 400, 01328 Dresden, Germany

4. Institute of Physics, Technische Universität Chemnitz, Reichenhainer Straße 70, 09126 Chemnitz, Germany

† Present Address: CIC Nanogune Consolider, Tolosa Hiribidea 76, 20018 Donostia-San Sebastian, Spain

* Corresponding Author: simone.pisana@lassonde.yorku.ca

Figure S1 shows the sensitivity analysis for the sample ML-3 at 1.25 μm beam offset, where the absolute difference in the modeled thermal phase for each parameter of interest is changed by 10%. Sensitivity analysis shows that by using a frequency range of 300 kHz to 8 MHz, the sensitivity to the parameter of interest is reasonably large compared to the phase noise ($\lesssim$ 0.2 deg), rendering anisotropic thermal conductivity measurements possible. We note that the sensitivity to $G_{SiO2/Si}$ is comparable to $k_r$. $G_{SiO2/Si}$, extracted from measurements made on the same substrate coated with Al, was kept constant for the analysis of the ML samples. The obtained $G_{SiO2/Si}$ = 27.02 ± 0.78 MW/m$^2$K is in agreement with our previous measurements [S1]. Furthermore, we are using a constant value of 250 MW/m$^2$K as the effective conductance across the ML/$SiO_2$ layers ($G_{ML/SiO2}$), in agreement with reference [S2]. Isotropic thermal conductivities of $k_{SiO2}$ = 1.32 W/mK & $k_{Si}$ = 145 W/mK and volumetric heat capacities of $C_{SiO2}$ = 1.59 MJ/m$^3$K & $C_{Si}$ = 1.64 MJ/m$^3$K have been used for the $SiO_2$ and Si layers.

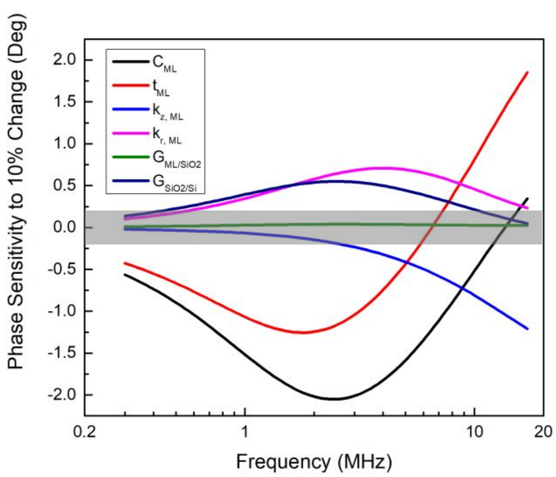


**Figure S1.** Thermal phase sensitivity to 10% change in the parameters labeled for sample ML-3 ($t_{Pt}$ = 2.8nm, $t_{Co}$ = 1.6nm, $q$ = 32) at 1.25 μm beam offset. The grey region is within the experimental phase noise of 0.2 deg.

To further explore how well we can distinguish the $k_z$ and $k_r$ fitted values, we present contours of uncertainty arising from correlation between $k_r$ and $k_z$. This is performed by calculating the mean square error between model and measured data for combinations of $k_r$ and $k_z$ values using the mean square error

$$\sigma = \frac{1}{p}\sum_{i=1}^{p}\left(\frac{X_{m,i} - X_{d,i}}{X_{d,i}}\right)^2$$

in this expression, $p$ is the number of frequency points and $X_{m,i}$ and $X_{d,i}$ represent phase values from the model and the measurement at the $i$-th frequency point, respectively [S3]. Figure S2 shows the contours of $k_r$ and $k_z$ combinations for ML-1 (with the largest correlation between $k_r$ and $k_z$) and ML-5 (with the smallest correlation between $k_r$ and $k_z$), which produce a standard deviation smaller than $2\sigma_{min}$, where $\sigma_{min}$ represents the best fit. The correlation for ML-1 is present, as evident by the contour's diagonal. However, the correlations are restricted to narrow ranges in $k_r$ and $k_z$ for good fits, rendering the extracted values meaningful. The correlation for ML-5 is weak, indicating the fit to these two parameters is relatively independent. However, the contours are broad for $k_z$, indicating a larger uncertainty for the extraction of this parameter. This is due to the low thermal resistance for this ML sample having the fewest number of interfaces.

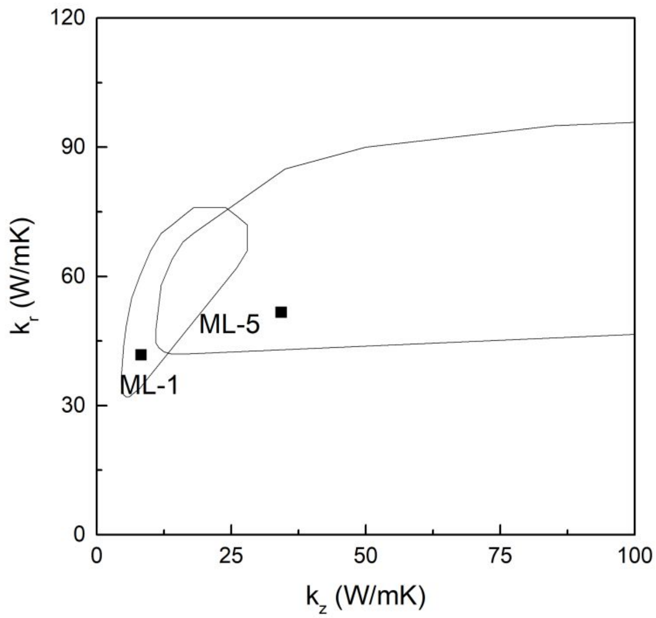


**Figure S2.** Contour plots of the correlation in the fitted values for $k_r$ and $k_z$ for ML-1 ($t_{Pt}$ = 0.7nm, $t_{Co}$ = 0.4nm, $q$ = 128) and ML-5 ($t_{Pt}$ = 44.8nm, $t_{Co}$ = 25.6nm, $q$ = 2). The contour lines map the combinations of $k_r$ and $k_z$ values that yield $2\sigma_{min}$, twice the mean square error obtained for the best fits (symbols).

The FDTR analysis presented in this work assumes that heat is deposited at the surface of the sample, while due to the finite absorption depth of laser light, this assumption is not always appropriate. To check the effect of this assumption, the top 10 nm of the ML was replaced with a 1 nm layer with ten times the volumetric heat capacity and ten times thermal conductivity of the MLs [S4]. This mimics light energy absorption within the optical absorption depth of the metallic multilayer. This yields the TBC values reported in Figure S3. Although a shift in TBC values exists when the finite absorption of light is considered (Figure S3 vs Figure 3 in the main text), a similar trend can be seen where the derived TBC values depend on the interface density and surpass EDMM and MTL predictions.

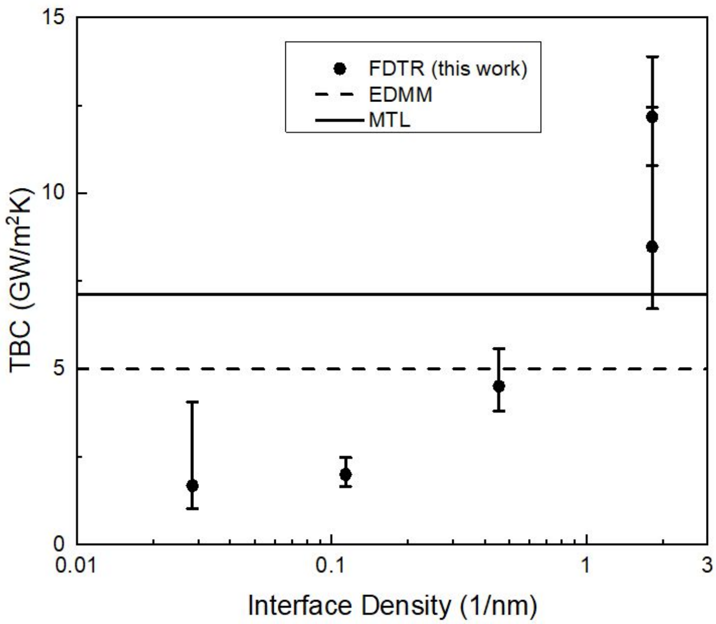


**Figure S3.** Pt/Co thermal boundary conductance extracted from FDTR fits, considering light's finite absorption depth, compared with the predictions from EDMM and MTL.

[S1] Shahzadeh, M.; Rahman, M.; Hellwig, O.; Pisana, S. High-frequency measurements of thermophysical properties of thin films using a modified broad-band frequency domain thermoreflectance approach. *Review of Scientific Instruments* **2018**, *89* (8), 084905.

[S2] Kimling, J.; Philippi-Kobs, A.; Jacobsohn, J.; Oepen, H.P.; Cahill, D.G. Thermal conductance of interfaces with amorphous $SiO_2$ measured by time-resolved magneto-optic Kerr-effect thermometry. *Physical Review B* **2017**, *95* (18), 184305.

[S3] Scott, E.A.; Smith, S.W.; Henry, M.D.; Rost, C.M.; Giri, A.; Gaskins, J.T.; Fields, S.S.; Jaszewski, S.T.; Ihlefeld, J.F.; Hopkins, P.E. Thermal resistance and heat capacity in hafnium zirconium oxide (Hf1–xZrxO2) dielectrics and ferroelectric thin films. *Applied Physics Letters* **2018**, *113* (19), 192901.

[S4] Cahill, D.G. Analysis of Heat Flow in Layered Structures for Time-Domain Thermoreflectance. *Review of Scientific Instruments* **2004**, *75* (12), 5119–5122.